

## HEMATOPOIESIS AND STEM CELLS

# Asrij/OCIAD1 suppresses CSN5-mediated p53 degradation and maintains mouse hematopoietic stem cell quiescence

Saloni Sinha,<sup>1</sup> Tirath Raj Dwivedi,<sup>1</sup> Roja Yengkhom,<sup>1</sup> Venkata Anudeep Bheemsetty,<sup>1</sup> Takaya Abe,<sup>2</sup> Hiroshi Kiyonari,<sup>2,3</sup> K. VijayRaghavan,<sup>4</sup> and Maneesha S. Inamdar<sup>1,5</sup>

<sup>1</sup>Jawaharlal Nehru Centre for Advanced Scientific Research, Bangalore, India; <sup>2</sup>Genetic Engineering Team and <sup>3</sup>Animal Resource Development Unit, RIKEN Center for Life Science Technologies, Kobe, Japan; <sup>4</sup>National Centre for Biological Sciences, Bangalore, India; and <sup>5</sup>Institute for Stem Cell Biology and Regenerative Medicine, Gandhi Krishi Vignana Kendra, Bangalore, India

## KEY POINTS

- **Asrij interacts with COP9 signalosome subunit CSN5 to prevent MDM2-mediated p53 degradation and maintains mouse bone marrow HSC quiescence.**
- **Asrij is a novel regulator of wild-type p53 stability in HSCs and could help design targeted therapies for myeloproliferative disease.**

**Inactivation of the tumor suppressor p53 is essential for unrestrained growth of cancers. However, only 11% of hematological malignancies have mutant p53. Mechanisms that cause wild-type p53 dysfunction and promote leukemia are inadequately deciphered. The stem cell protein Asrij/OCIAD1 is misexpressed in several human hematological malignancies and implicated in the p53 pathway and DNA damage response. However, Asrij function in vertebrate hematopoiesis remains unknown. We generated the first *asrij* null (knockout [KO]) mice and show that they are viable and fertile with no gross abnormalities. However, by 6 months, they exhibit increased peripheral blood cell counts, splenomegaly, and an expansion of bone marrow hematopoietic stem cells (HSCs) with higher myeloid output. HSCs lacking Asrij are less quiescent and more proliferative with higher repopulation potential as observed from serial transplantation studies. However, stressing KO mice with sublethal  $\gamma$  irradiation or multiple injections of 5-fluorouracil results in reduced survival and rapid depletion of hematopoietic stem/progenitor cells (HSPCs) by driving them into proliferative exhaustion. Molecular and biochemical analyses revealed increased polyubiquitinated protein levels, Akt/STAT5 activation and COP9 signalosome subunit 5 (CSN5)-mediated p53 ubiquitination, and degradation in KO HSPCs. Further, we show that Asrij sequesters CSN5 via its conserved OCIA domain, thereby preventing p53 degradation. In agreement, Nutlin-3 treatment of KO mice restored p53 levels and reduced high HSPC frequencies. Thus, we provide a new mouse model resembling myeloproliferative disease and identify a posttranslational regulator of wild-type p53 essential for maintaining HSC quiescence that could be a potential target for pharmacological intervention. (*Blood*. 2019;133(22):2385-2400)**

## Introduction

Bone marrow (BM) hematopoietic stem cells (HSCs) self-renew and can differentiate to all blood lineages to replenish the blood system after immune challenge, radiation, or chemotherapy.<sup>1,2</sup> The BM hematopoietic niche is a specialized microenvironment that houses HSCs and plays important roles in regulating their quiescence, self-renewal, and fate specification.<sup>3</sup> At the apex of the hematopoietic hierarchy is a pool of dormant HSCs<sup>4</sup> whose fundamental property is quiescence. The interplay of several cell-intrinsic (transcription factors, signal transducers, epigenetic regulators) and cell-extrinsic (niche-induced) factors maintains quiescence and protects the HSC pool from premature exhaustion.<sup>5,6</sup> Stringent control of HSC proliferation and differentiation maintains steady-state hematopoiesis.<sup>7</sup> Despite

considerable progress, molecular processes that regulate HSC quiescence are incompletely characterized. Hence, identification of novel regulators of HSCs is crucial.

The tumor suppressor p53 is expressed at high levels in HSCs<sup>8</sup> and maintains self-renewal and quiescence by regulating the activity of various downstream targets such as *p21*, *gfi1*, and *necdin*.<sup>9</sup> Approximately, 50% of human sporadic cancers have inactivating mutations and deletions in *TP53*.<sup>10</sup> However, this is uncommon in hematological malignancies,<sup>11,12</sup> occurring in only 8% of acute myeloid leukemia (AML) cases.<sup>13</sup> According to the European Leukemia Net Classification, nonmutational wild-type p53 (*wtp53*) dysfunction is found in nearly all AML subsets.<sup>14</sup> Although p53 function in regulation of HSC quiescence, fate,

and behavior is well-characterized, relatively little is known about events leading to nonmutational wtp53 dysfunction.<sup>14</sup> Stability and activity of p53 are determined primarily by its posttranslational modifications, such as ubiquitination, phosphorylation, and acetylation.<sup>15</sup> Hence, a deeper understanding of posttranscriptional regulation of p53 in hematopoiesis is essential.

The tumor invasion/progression protein, *Asrij*/OCIAD1, is mutated<sup>16,17</sup> or shows altered expression in several blood disorders<sup>18</sup> ([http://servers.binf.ku.dk/bloodspot/?gene=OCIAD1&dataset=all\\_mile](http://servers.binf.ku.dk/bloodspot/?gene=OCIAD1&dataset=all_mile)), contains p53-binding sites<sup>19</sup> and is implicated in DNA damage signaling.<sup>20</sup> Hence, we chose to study its role in mammalian hematopoiesis.

*Asrij*/OCIAD1, a member of the Ovarian Carcinoma Immunoreactive Antigen (OCIA) domain family,<sup>21</sup> was first identified as a gene expressed in mouse embryonic stem (ES) cells and the developing blood vasculature.<sup>22</sup> *Asrij* maintains mouse ES cell pluripotency.<sup>23</sup> In *Drosophila* hematopoiesis, *Asrij* maintains the niche and negatively regulates blood progenitor differentiation.<sup>24</sup> Interestingly, mouse and *Drosophila* *Asrij* are true homologs as mouse *Asrij* can maintain the stem cell state in *Drosophila* owing to the conserved activity of its N-terminal OCIA domain.<sup>23</sup> To elucidate the role of *Asrij* in vertebrates, we generated the first *asrij* null mutant mice by Cre-loxP-mediated deletion and analyzed the consequences of *asrij* depletion. We show that loss of *Asrij* leads to defective BM hematopoiesis with increased accumulation of polyubiquitinated proteins, increased activation of Akt/STAT5, and reduced stability of wtp53, resulting in HSC expansion and a myeloproliferative disorder. Our findings demonstrate that *Asrij* is essential for maintaining HSC quiescence.

## Methods

### Generation and validation of *asrij* KO mice

C57BL6/J was used as the wild-type strain. Exon 6 of the *asrij* locus (chromosome 5: 22886700-22887300) was floxed by homologous recombination using a targeting vector in TT2 mouse ES cells. Recombinants selected by G418 resistance and genomic analyses with Southern hybridization were microinjected into ICR (Cd-1) 8-cell stage embryos. Resulting chimeras were crossed to C57BL/6N to obtain germ-line transmitted recombinant progeny. Heterozygous recombinant mice (*asrij*<sup>fllox/+</sup>) were bred to homozygosity and crossed with *CMV-Cre*<sup>+25</sup> mice for ubiquitous deletion of *asrij* or to *Vav-iCre*<sup>+26</sup> for deletion in the hematopoietic system. Heterozygotes (*asrij*<sup>fllox/+</sup>; *CMV-Cre*<sup>+</sup>) were bred to generate *asrij* knockout (KO) mice (see supplemental Methods, available on the *Blood* Web site).

### Statistical analysis and quantification

Means  $\pm$  standard errors of the mean were plotted as graphs using SigmaPlot11.0. Statistical comparison of complete blood cell counts of mice belonging to different age-matched groups and mice treated with 5-fluorouracil (5-FU) was done using repeated measures analysis of variance (ANOVA) in STATISTICA 7. Statistical comparisons for cell percentages or absolute cell counts, colony number or diameter, spleen weights, transcript, and protein expression levels were done using ANOVA: single factor using Analysis ToolPak in Microsoft Excel 2007. Survival analysis of mice was done using Kaplan-Meier test in SPSS.

Statistically significant differences were indicated by \* $P < .05$ , \*\* $P < .01$ , and \*\*\* $P < .001$ .

## Results

### *Asrij* is expressed in BM hematopoietic populations

*Asrij* expression is primarily restricted to the hematopoietic system in *Drosophila*.<sup>24</sup> Hence, we investigated it in the mouse hematopoietic system. Data mining of the mouse RNA-Seq expression database ([http://blood.stemcells.cam.ac.uk/single\\_cell\\_atlas.html#data](http://blood.stemcells.cam.ac.uk/single_cell_atlas.html#data))<sup>27</sup> showed high *asrij* expression in long-term HSCs (LT-HSCs) and progenitor subpopulations (supplemental Figure 1A). Expression profiling of wild-type BM revealed that *asrij* transcript is highly expressed in LT-HSCs, short-term HSCs (ST-HSCs), and multipotent progenitors (MPPs) as compared with unfractionated BM (supplemental Figure 1B). Flow cytometry analysis showed *Asrij* expression in about  $75.3 \pm 5.2\%$  of the BM (supplemental Figure 1C), which included LT-HSCs ( $46.8 \pm 2.84\%$  of Lineage<sup>-low</sup> Sca1<sup>+</sup> c-Kit<sup>+</sup> [LSK]-CD150<sup>+</sup> CD48<sup>-</sup>) (Figure 1A), HSPCs ( $98.2 \pm 0.9\%$  of LSK), and myeloid ( $92.4 \pm 2.3\%$  of CD11b<sup>+</sup>) and lymphoid ( $76.8 \pm 5.4\%$  of CD19<sup>+</sup>) lineages (supplemental Figure 1C). In HSPCs, *Asrij* localized to cytoplasmic puncta positive for endosomal markers Rab4, Rab5, and Rab11 and mitochondrial marker CoxIV (Figure 1B). This suggested a possible role for *Asrij* in HSCs.

### *asrij* KO mice develop a myeloproliferative disorder

In *Drosophila*, *Asrij* maintains postembryonic blood progenitors and suppresses their differentiation.<sup>24</sup> Hence, we generated *asrij* floxed mice (see "Methods"; Figure 1C; supplemental Figure 1D) to investigate the consequences of *asrij* deletion (supplemental Figure 1E-I) on steady-state hematopoiesis. Mice lacking a single copy of *asrij* (*asrij*<sup>+/-</sup>; supplemental Figure 2A) expressed much reduced levels of *Asrij* compared with control (supplemental Figure 1B-C) and showed a modest increase in red blood cells and platelets only from 6 months of age, with no significant difference in HSPC frequencies or spleen sizes (supplemental Figure 2D-F). However, deletion of both alleles of *asrij* (*asrij*<sup>-/-</sup>; KO) caused significantly increased peripheral blood (PB) cell counts in young mice (2-4 months), with a progressive increase in counts with age (Figure 1D). Flow cytometry showed increased percentages of neutrophils and granulocytes (Gr1<sup>+</sup>), monocytes, and macrophages (CD11b<sup>+</sup>), and reduced percentages of B-cells (CD19<sup>+</sup>) and T cells (CD3<sup>+</sup>) in 6-month-old KO mice (supplemental Figure 3A). KO mice had significantly increased BM cellularity at 2 and 6 months of age compared with controls (supplemental Figure 3B). Compared with control, KO mice showed significantly increased percentages and absolute numbers of myeloid-enriched progenitor population (Lin<sup>-</sup> c-Kit<sup>+</sup>), HSPCs, LT-HSCs (LSK-CD150<sup>+</sup>CD48<sup>-</sup>), ST-HSCs (LSK-CD150<sup>+</sup>CD48<sup>-</sup>), and MPP2s (LSK-CD150<sup>+</sup>CD48<sup>+</sup>), whereas MPP3s (LSK-CD150<sup>-</sup>CD48<sup>+</sup>) were fewer (Figure 1E-I). Similar results were obtained using the CD34/Flk2 marker combination (supplemental Figure 3C-D), confirming that *Asrij* depletion results in an expansion of HSC pools.

Percentages and absolute numbers of granulocyte-macrophage progenitors (GMPs) in the Lin<sup>-</sup> c-Kit<sup>+</sup> subpopulation as well as the CD11b<sup>+</sup> myeloid fraction were significantly increased in KO mice (Figure 1J-M), whereas common lymphoid progenitors and CD19<sup>+</sup> lymphoid fraction were significantly reduced (Figure 1K-M). In agreement with the HSC expansion and increased myeloid differentiation observed, immunoblotting showed increased

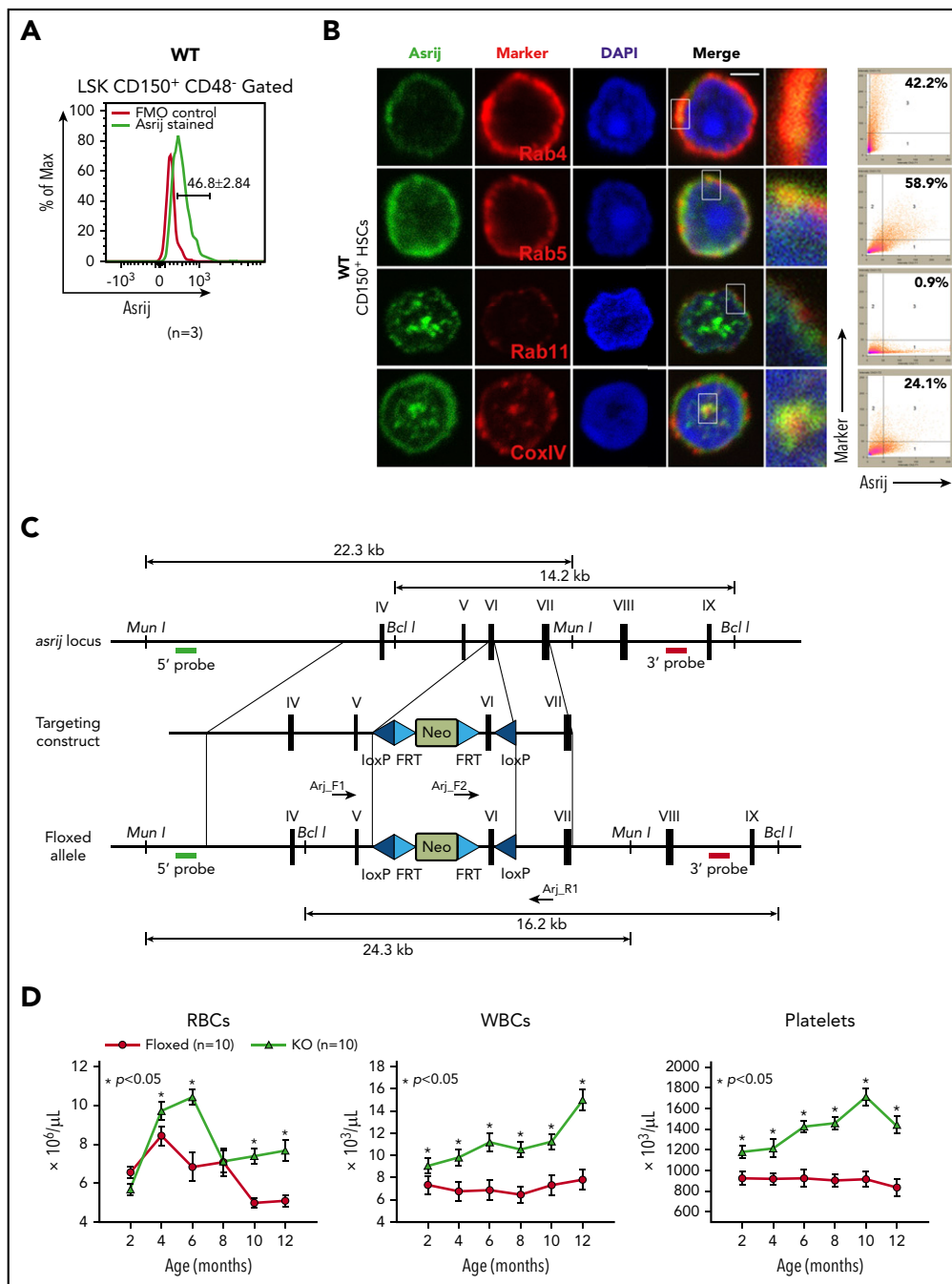


**Figure 1. *asrij* KO mice develop a myeloproliferative disorder.** (A) Flow cytometric detection of *Asrij* expression in LT-HSCs (LSK CD150<sup>+</sup>CD48<sup>-</sup>). Percentage of LT-HSCs positive for *Asrij* is detailed in the histogram overlay. Mean fluorescent intensity values for “FMO control” = 232 and “*Asrij* stained” = 506 (n = 3 wild-type mice). (B) HSCs (LSK CD150<sup>+</sup>) were immunostained with antibodies against *Asrij* (green), various endosome (Rab4, Rab5, Rab11), and mitochondrial (CoxIV) markers (red) and DAPI to mark nuclei (blue). Insets show magnified view of the boxed region. Graphs indicate extent of colocalization in a single confocal plane. Bar represents 2  $\mu$ m (n = 30 cells from 3 wild-type mice). (C) Schematic showing strategy for generation of floxed allele of *asrij* at exon 6. Black rectangles, exons; blue triangles, *loxP* sites; light blue triangles, *frt* sites; lime green rectangles, neomycin cassette; 5' probe and 3' probe, probes for Southern blotting; black arrows, genotyping primers (Arj\_F1, Arj\_F2, and Arj\_R1). (D-P) Floxed and KO cells were analyzed in all cases and are indicated in red and light green, respectively. (D) Graphs show change in PB cell counts (red blood cells, WBCs, and platelets) of floxed (red circles) and KO (green triangles) mice from 2 to 12 months of age. Statistically significant differences determined using repeated measures ANOVA are indicated (n = 10 mice per genotype). (E) Representative flow cytometry plots to show the frequency of Lin<sup>-</sup> cells, LKs, and LSKs at 6 months of age (n = 7 mice per genotype). (F) Graphs showing frequency of LKs and LSKs within BM and their absolute number per femur and tibia (n = 7 mice per genotype). (G) Flow cytometric analysis of the frequencies of LT-HSCs, ST-HSCs, and MPPs at 6 months of age, identified using SLAM markers CD150/CD48 (n = 7 mice per genotype). (H-I) Graphs showing frequency of LT-HSCs, ST-HSCs, MPP2, and MPP3 within LSK and their absolute number per femur and tibia (n = 7 mice per genotype). (J) Flow cytometric analysis of CMPs, GMPs, and MEPs at 6 months of age (n = 10 mice per genotype). (K-L) Graphs showing frequency of CMPs, GMPs, MEPs and common lymphoid progenitors within BM and their absolute number per femur and tibia (n = 3 mice per genotype). (M) Graph representing frequency of BM CD11b<sup>+</sup> and CD19<sup>+</sup> subpopulations at 6 months of age (n = 3 mice per genotype). (F,H,I,K,L,M) Statistically significant differences for determined using ANOVA: single factor analysis are indicated. (N) Hematoxylin and eosin staining of BM sections from 2-month-old mice. Right panels show magnified view of the boxed area. Arrow points to osteolytic lesions in KO bone (n = 3 mice per genotype). Bar represents 1 mm. (O) Graph showing change in spleen weight across different age groups. Representative spleen images are shown above the respective age groups. Bar represents 0.5 cm or 1 cm, as indicated (n > 7 mice per genotype). Bars denote standard error of mean. \*P < .05, \*\*P < .01, \*\*\*P < .001. LK, LIN<sup>-</sup>c-Kit<sup>+</sup>Sca-1<sup>-</sup>; LSK, LIN<sup>-</sup>c-Kit<sup>+</sup>Sca-1<sup>+</sup>.

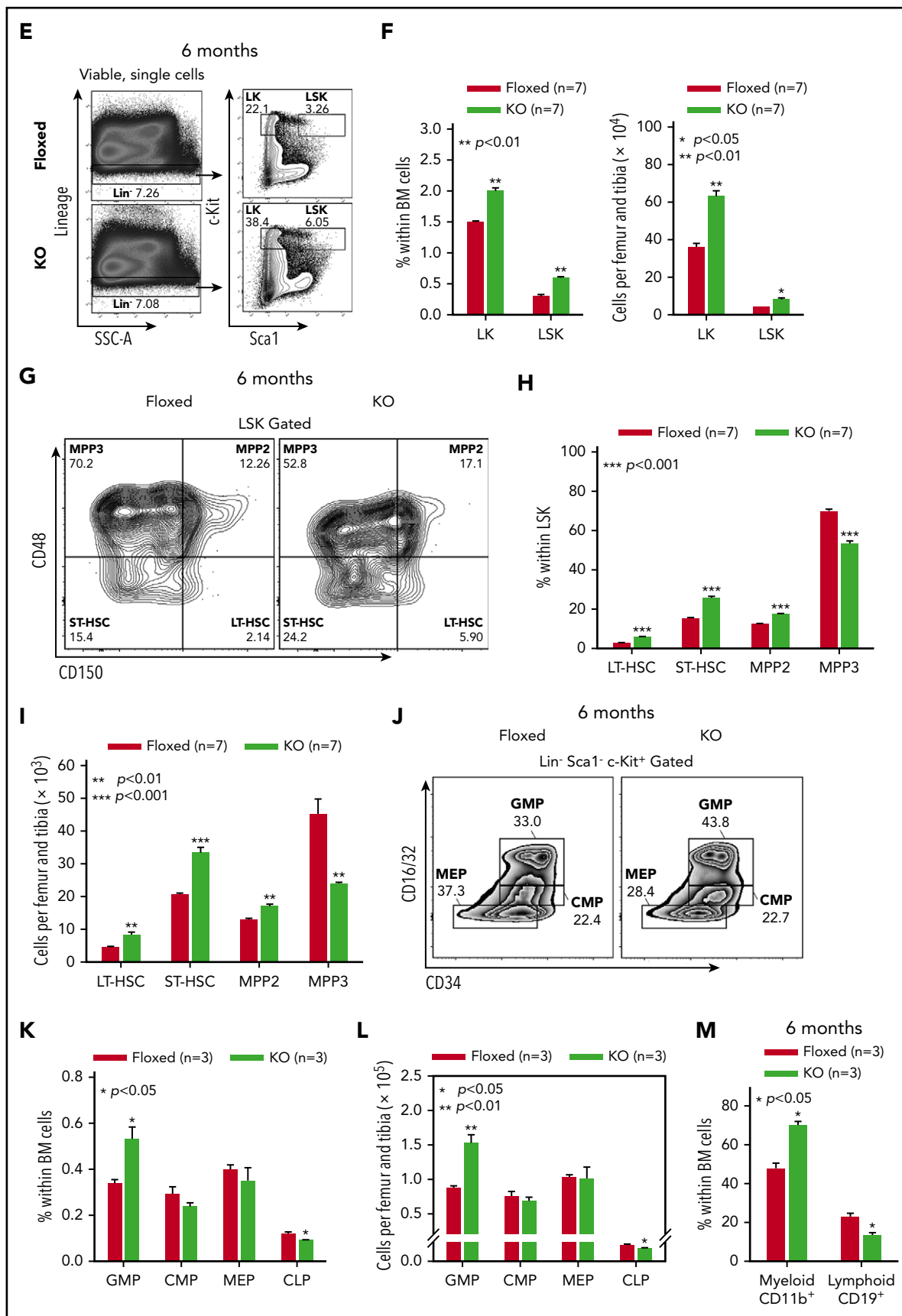
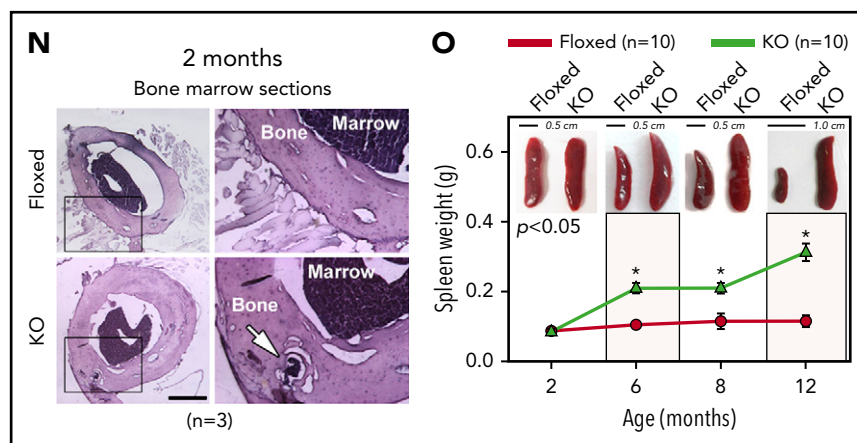


Figure 1. (Continued).

Figure 1. (Continued).



activation of critical downstream signaling molecules such as Akt (S473) and STAT5 (Y694) in KO HSPCs (supplemental Figure 3E-F).<sup>28</sup> Bone histology showed myeloid infiltration of cells into femurs of 2-month-old KO mice (Figure 1N). KO mice also developed splenomegaly (Figure 1O) and had enlarged splenic follicles and infiltration in other tissues such as liver and kidney by 12 months of age (supplemental Figure 3G). Moreover, KO mice showed reduced lifespan and are more prone to developing kyphosis (supplemental Figure 4; supplemental Results). Taken together, *Asrij* depletion causes aberrant HSC expansion and a myeloproliferative disorder.

### ***Asrij* regulates HSC quiescence and proliferation**

To identify how *Asrij* maintains the stem cell compartment, we examined the cell-cycle status of KO HSPCs and HSCs. Hoescht 33342/Pyronin-Y staining showed that KO HSPCs including LT-HSCs, ST-HSCs, and MPPs had significantly reduced cells in G<sub>0</sub>, as compared with control subpopulations (Figure 2A). Ki-67/7-aminoactinomycin D (7-AAD) staining confirmed the increased proliferative potential of KO HSPCs and HSCs (Figure 2B). This was additionally confirmed by in vitro OP9 coculture experiments with LSK-CD34<sup>-/-</sup> subpopulations, which showed that KO HSPCs formed larger colonies that were also greater in number compared with control (Figure 2C). In addition, significantly increased HSPC percentages were observed in spleen and PB of KO mice (Figure 2D). In a methylcellulose colony-forming unit (CFU) assay, BM cells and splenocytes from 6-month-old mice showed a significant increase in the colony frequencies and sizes of CFU-GMs (granulocyte/macrophage), whereas burst-forming unit erythroid, and CFU-granulocyte/erythroid/macrophage/megakaryocyte colonies were comparable to control (Figure 2E-F). These data support an intrinsic role for *Asrij* in regulating HSC quiescence and proliferation.

### ***Asrij* contributes to the repopulation ability of HSCs and aids in recovery from hematopoietic stress**

Aberrant hematopoietic phenotypes in KO mice could be due to defects in HSCs or in the BM microenvironment that provides the stem cell niche. To evaluate whether KO BM could reconstitute the hematopoietic system of lethally irradiated mice, we performed serial noncompetitive BM transplantation (BMT) (see "Methods"; Figure 3A). Transplanted recipients were assessed for donor contribution to confirm successful engraftment of CD45.2<sup>+</sup> cells. Primary transplants injected with KO BM showed significantly increased white blood cells (WBCs) and platelets,

had significant HSPC expansion and also showed splenomegaly (Figure 3B-D), reminiscent of the hematopoietic phenotypes observed in KO mice. Similarly, secondary transplants injected with KO BM also developed phenotypes similar to the primary transplants (Figure 3E-G). Thus, compared with control, KO BM cells have a higher in vivo reconstitution ability and the KO phenotypes are transplantable. Further, to assess the contribution of the BM microenvironment to the KO hematopoietic phenotype, we performed reciprocal BMT (see "Methods"; supplemental Figure 5A). KO mice injected with CD45.1<sup>+</sup> BM did not show any difference in PB counts, HSPC frequencies, or spleen weights as compared with floxed mice that were similarly injected (supplemental Figure 5B-D). This indicates that absence of *Asrij* in the BM microenvironment does not affect the repopulation ability of wild-type HSPCs and that the KO niche can support hematopoiesis. Conversely, similar to ubiquitous KO, hematopoietic-specific deletion of *asrij* (*asrij*<sup>fl<sup>ox</sup>/fl<sup>ox</sup></sup>; *Vav-iCre*<sup>+</sup> [*asrij*<sup>CKO</sup>]) leads to increased PB cell counts and HSPC frequencies, confirming that *Asrij* expression in hematopoietic lineages is essential for regulating hematopoiesis (supplemental Figure 6A-F).

The reduced quiescence of KO HSCs suggested that KO mice may be more susceptible to stress. To test the contribution of *Asrij* to stress-induced hematopoiesis, we exposed control and KO mice to radiation and chemically induced stress. Although all control mice subjected to a sublethal dose (6.5 Gy) of  $\gamma$  irradiation survived beyond 25 days, similarly irradiated KO mice showed significantly reduced survival with ~50% of the mice succumbing to radiation within 15 days (Figure 3H). Both control and KO mice showed distinct leukopenia and erythropenia phenotypes, 7 days postirradiation, with KO mice showing significantly lower PB cell counts (Figure 3I). Consistent with this observation, 12 days postirradiation, KO BM had significantly reduced HSPC percentages (Figure 3J). Ki-67/7-AAD staining 12 days postirradiation showed significantly increased percentage of KO HSCs in the S/G<sub>2</sub>/M phases (Figure 3K), compared with control, indicating increased radiation-induced proliferation drives KO HSPCs toward premature exhaustion.

Chemical stress was achieved by injecting 5-FU, a cell cycle-specific cytotoxic agent that preferentially targets proliferating HSPCs. Mice repeatedly injected with 150 mg/kg of 5-FU, weekly, for a period of 3 weeks, were assayed for survival and PB cell

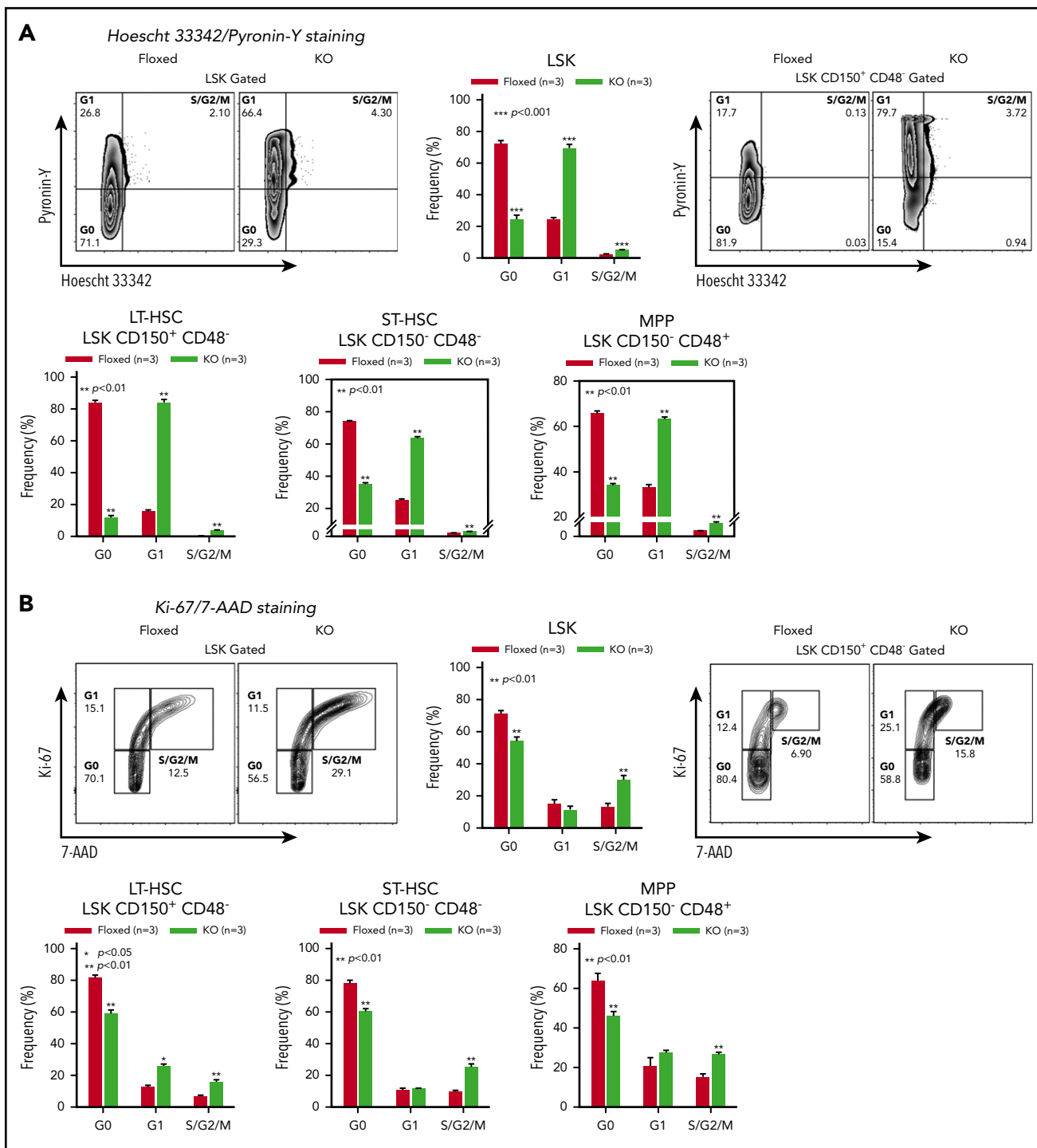


**Figure 2. Asrij depletion significantly reduces quiescence and increases proliferation of HSCs.** Floxed and KO cells were analyzed in all cases and are indicated in red and light green, respectively. (A) Representative Hoescht 33342/Pyronin-Y flow cytometric plots and graphs showing the cell-cycle distribution of HSPCs, LT-HSCs, ST-HSCs, and MPPs ( $n = 3$  mice per genotype). (B) Cell proliferation analysis using Ki-67/7-AAD staining of HSPCs, LT-HSCs, ST-HSCs, and MPPs ( $n = 3$  mice per genotype). (C) Representative images of OP9-HSPC cocultures showing colonies (red arrows) formed by HSPC (LSK-CD34<sup>-</sup> and LSK-CD34<sup>+</sup>) subpopulations. Bar represents 50  $\mu\text{m}$ . Graphs quantify number of colonies formed and number of cells/colony ( $n = 3$  mice per genotype). (D) Flow cytometric analysis and quantification of the HSPC frequencies in spleen and PB ( $n = 4$  mice per genotype). CFU-C assay to test the differentiation potential of (E) BM cells and (F) splenocytes harvested from 6-mo-old mice under erythromyeloid promoting conditions ( $n = 3$  mice per genotype). (E) Graphs show relative distribution of total, BFU-E, CFU-GM, and CFU-granulocyte/erythroid/macrophage/megakaryocyte colonies scored based on their morphology and colony diameter. (F) Graphs show colony percentage and colony diameter of CFU-GMs formed by splenocytes. Statistically significant differences identified using ANOVA: single factor analysis are indicated. Error bars denote standard error of mean. \* $P < .05$  and \*\* $P < .01$ .

counts. KO mice showed significantly increased lethality and reduced WBCs (Figure 3L-M) when compared with similarly treated controls, indicating that Asrij deletion sensitizes mice to

hematopoietic ablation. Taken together, our analysis shows that Asrij is essential for mediating hematopoietic recovery after exposure to stress.

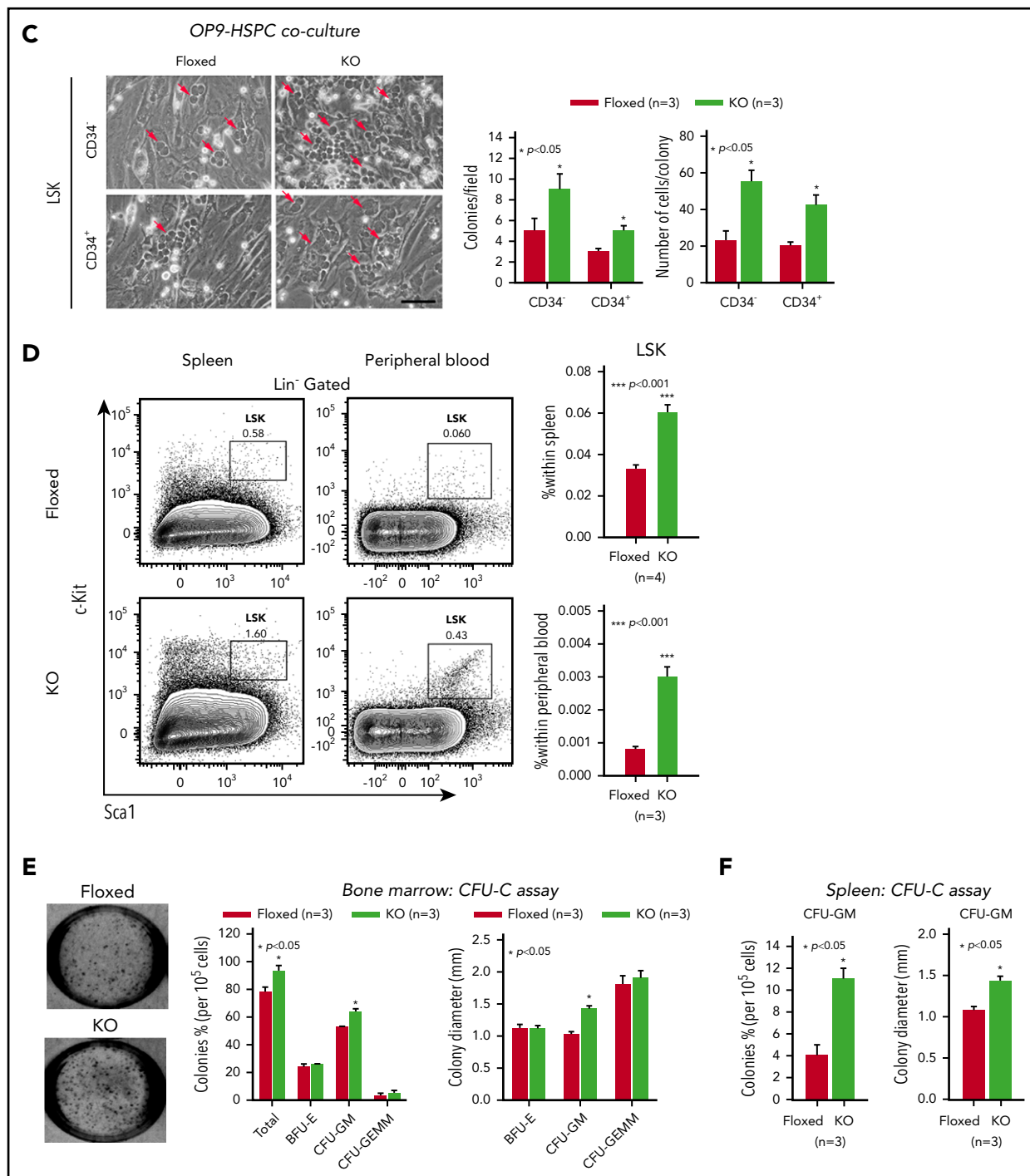
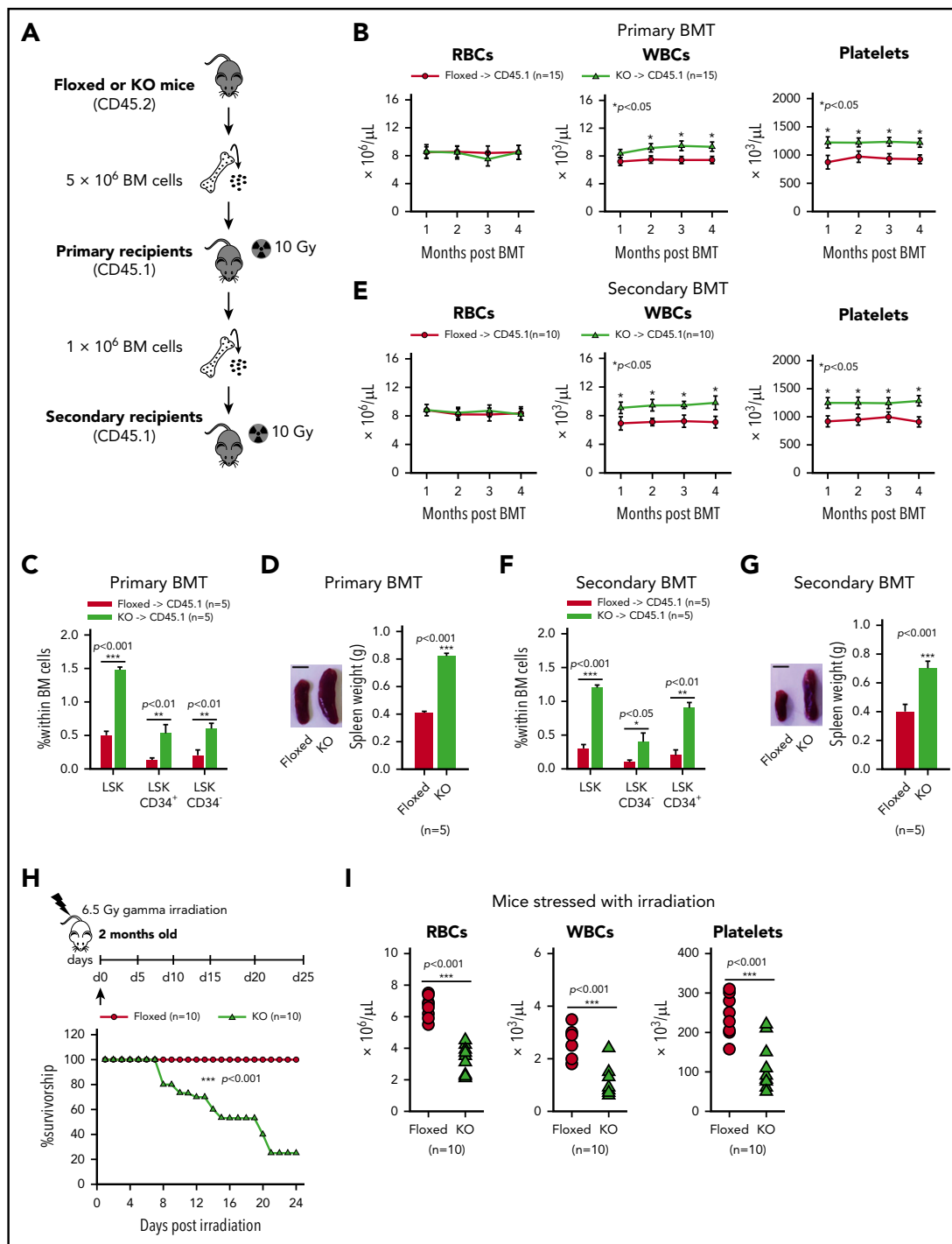


Figure 2. (Continued).

### Increased p53 degradation and DNA damage in *asrij* KO HSPCs

Tumor suppressors play important roles in maintaining hematopoiesis under both normal and stress conditions.<sup>9,29-33</sup> Because *Asrij* downregulation is linked to p53 and DNA damage pathways<sup>34</sup> and KO mice have an HSPC expansion phenotype, similar to *Trp53* null mice,<sup>35-38</sup> we checked the status of p53 and DNA damage in KO mice. The *Trp53* exon sequence showed no mutation, including the cancer-associated mutation hotspots (codons 245, 248, and 273; data not shown) and transcript level was unchanged (Figure 4A).

However, in KO HSPCs, p53 protein levels were significantly reduced suggesting that *Asrij* regulates p53 posttranscriptionally (Figure 4B). Further, expression of pro-apoptotic p53 targets *puma* and *noxa* was significantly reduced, whereas *p21*, *bcl2*, *gga1*, *gfi1*, and *neccin* were unaltered (Figure 4C). In agreement with this, KO LT-HSCs and ST-HSCs showed significantly reduced percentages of early (Annexin V<sup>+</sup>/7-AAD<sup>-</sup>) and late (Annexin V<sup>+</sup>/7-AAD<sup>+</sup>) apoptotic cells compared with control (Figure 4D-F). Importantly, KO HSPCs showed reduced apoptosis compared with control, both in vivo and ex vivo after short-term culture



**Figure 3. *Asrij* depletion results in increased repopulation ability and affects hematopoietic recovery from stress.** Floxed and KO cells were compared in all cases and are indicated in red and light green, respectively. (A) Schematic representation of the transplantation study. A total of  $5 \times 10^6$  BM cells harvested from 6-month-old (CD45.2<sup>+</sup>) *asrij* floxed or KO mice were injected into lethally irradiated (9.5 Gy) 2-month-old CD45.1 mice. These CD45.1 mice (primary transplants) were analyzed for PB cell counts at monthly intervals. Four months after transplantation,  $1 \times 10^6$  BM cells harvested from the primary transplants were injected into another set of lethally irradiated (9.5 Gy) CD45.1 recipients (secondary transplants), which were similarly analyzed. (B-E) Outcome of serial BMT assayed by analysis of (B,E) PB cell counts ( $n = 10$  mice per genotype) at monthly intervals after transplant, (C,F) HSPC frequencies ( $n = 3$  mice per genotype), and (D,G) spleen weights ( $n = 3$  mice per genotype) at 4 months posttransplant. Mice that received KO BM had significantly increased WBC and platelet counts, HSPC frequencies and spleen weights than those that received *asrij* floxed BM. (D,G) Bar represents 1 cm. Statistically significant differences for PB cell counts, identified using repeated measures ANOVA, and for HSPC frequencies and spleen weights, identified using ANOVA: single factor analysis, are indicated. (H) Kaplan-Meier survival analysis of 2-month-old mice stressed with sublethal dosage of  $\gamma$  irradiation (6.5 Gy,  $n = 10$  mice per genotype). \*\*\* $P < .001$ , generalized Wilcoxon test. (I) PB cell count analysis after irradiation ( $n = 10$  mice per genotype). (J) Flow cytometric analysis and quantification of HSPC frequencies after irradiation ( $n = 3$  mice per genotype). (K) Representative Ki-67/7-AAD flow cytometric plots and quantification showing the cell-cycle distribution of HSCs after irradiation ( $n = 3$  mice per genotype). (L) Kaplan-Meier survival analysis of 2-month-old mice stressed with 5-FU, weekly, for 3 weeks (150 mg/kg of mouse body weight,  $n = 10$  mice per genotype). \* $P < .05$ , generalized Wilcoxon test. (M) PB cell count analysis after 5-FU treatment shows significantly reduced WBCs in KO mice as compared with floxed controls ( $n = 10$  mice per genotype). Statistically significant differences for (I-K) identified using ANOVA: single factor analysis and for (M) identified using repeated measures ANOVA are indicated. Black arrow, time of stress administration to mice. Error bars denote standard error of mean. \* $P < .05$ , \*\* $P < .01$ , and \*\*\* $P < .001$ .



Figure 3. (Continued).

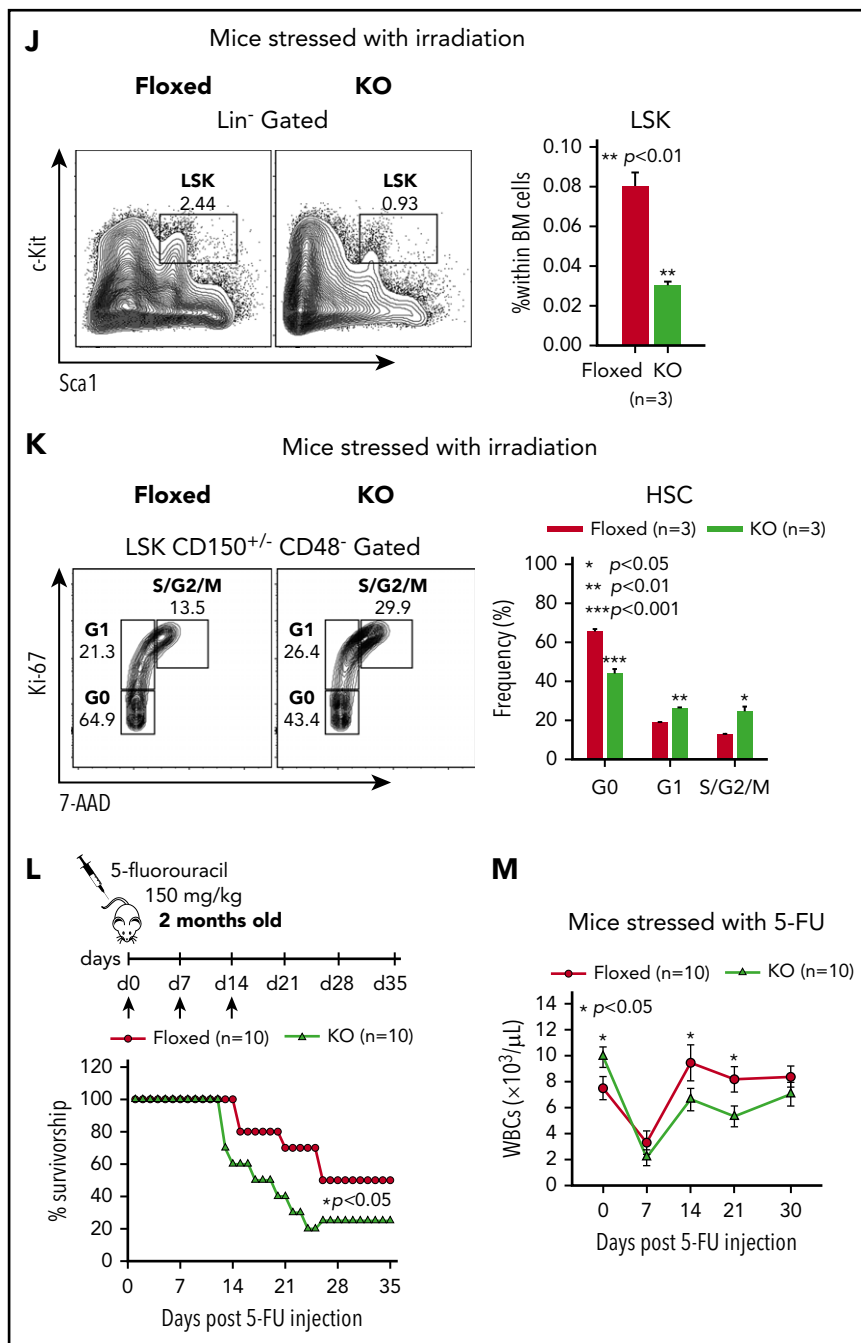


(Figure 4G). p53 also orchestrates a variety of DNA damage responses.<sup>39</sup> Immunoblotting analysis showed higher γH2AX levels in KO HSPCs, suggesting increased accumulation of DNA damage upon *Asrij* depletion (Figure 4H).

The ubiquitin-proteasome system plays critical roles in regulating the levels and activity of p53.<sup>40,41</sup> Hence, reduced p53 in KO HSPCs could be due to aberrant ubiquitination resulting in increased p53 degradation. Immunostaining revealed increased accumulation of polyubiquitinated proteins in KO BM cells suggesting this machinery is deregulated in the absence of *Asrij* (Figure 5A). Immunopulldown followed by immunoblotting showed increased levels of ubiquitinated-wtp53 in KO BM as compared with control, indicating increased p53 degradation

(Figure 5B). Thus, *Asrij* depletion results in reduced p53 levels and increased DNA damage in HSPCs.

### ***Asrij* interacts with CSN5 and negatively regulates its levels in HSPCs**

To probe further into the mechanism that drives HSPC expansion phenotype in *asrij* KO mice, we looked for other mouse models with similar phenotypes of aberrant hematopoiesis. Transgenic mice that overexpress the COP9 signalosome (CSN) component CSN5 were also reported to develop an HSPC expansion phenotype at ~6 months age.<sup>42</sup> CSN5 is the fifth subunit of the COP9 signalosome, an evolutionary conserved protein complex that regulates the fate of the ubiquitin-proteasome pathway.<sup>43-45</sup> Importantly, CSN5 is a negative regulator of p53.<sup>46</sup> Because KO

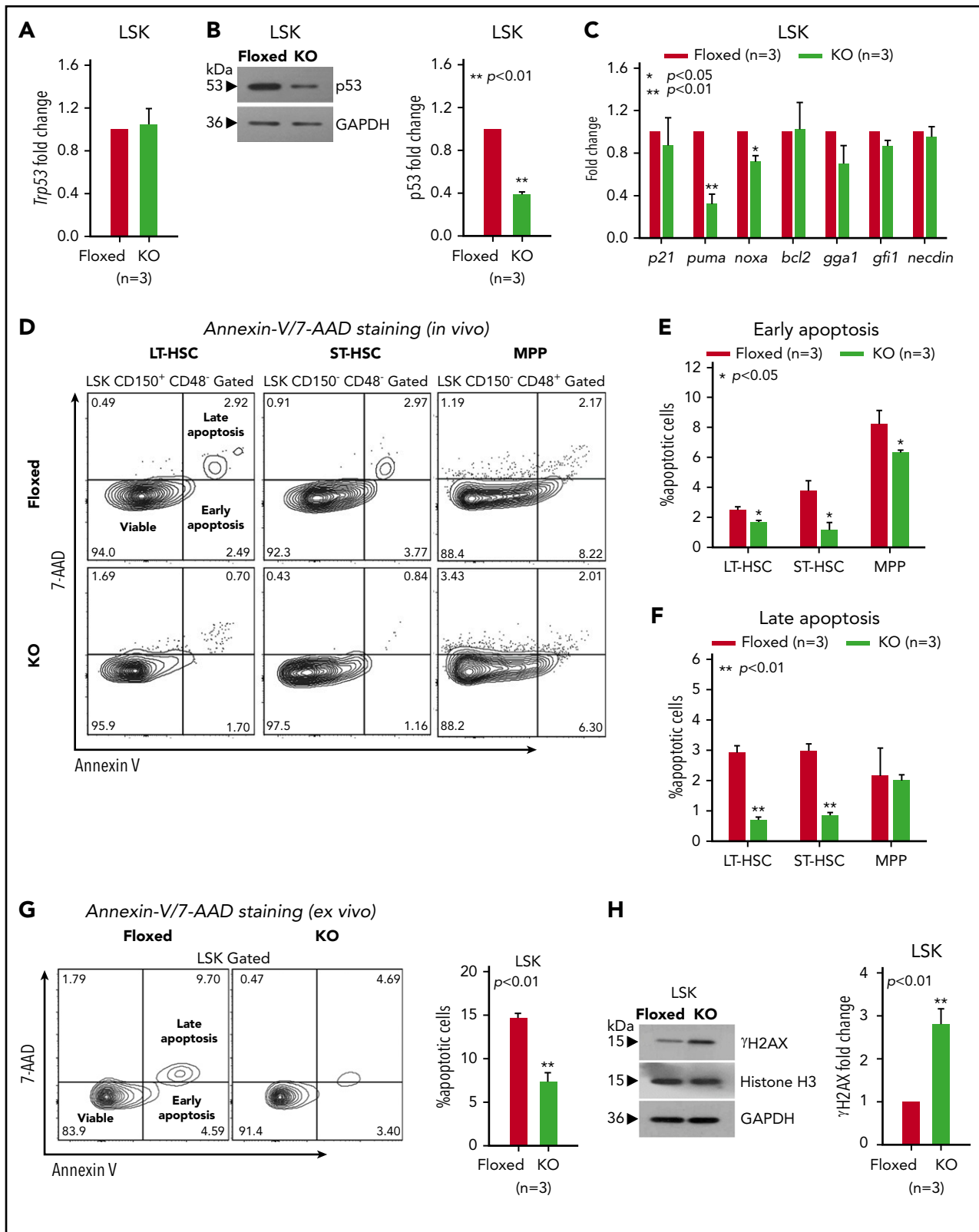


**Figure 4. *asrij* KO HSPCs have reduced p53 protein levels and increased DNA damage.** Floxed and KO cells from 2-month-old mice were compared in all cases (unless mentioned otherwise) and are indicated in red and light green, respectively. (A) RT-qPCR analysis for *p53* transcript levels and (B) immunoblot analysis for p53 protein levels in HSPCs. (C) RT-qPCR analysis for *p21*, *puma*, *noxa*, *bcl2*, *gga1*, *gfi1*, and *necdin* transcript levels in HSPCs. (D-G) Representative Annexin V/7-AAD flow cytometry plots and graphs showing significantly reduced percentages of early and late apoptotic cells in 6-month-old KO HSPCs compared with floxed controls, both in vivo and ex vivo after short-term culture. (H) Immunoblot analysis for  $\gamma$ H2AX protein levels to assess DNA damage in HSPCs. Histone H3 and GAPDH: loading controls. (A-H)  $n = 3$  mice per genotype for each experiment. Statistically significant differences in transcript and protein levels were determined using ANOVA: single factor analysis. Error bars denote standard error of mean. \* $P < .05$  and \*\* $P < .01$ . GAPDH, glyceraldehyde-3-phosphate dehydrogenase; RT-qPCR, reverse transcription quantitative polymerase chain reaction.

HSPCs had reduced wild-type p53 protein levels, we checked the status of CSN5 and found a significant upregulation in its transcript and protein expression (Figure 5C-D). Immunoblotting of *asrij*<sup>CKO</sup> BM revealed a similar perturbation of the CSN5-p53 signaling axis (supplemental Figure 7A-C). CSN5 stabilizes MDM2, the E3-ubiquitin ligase that ubiquitinates p53 and marks it for degradation.<sup>47</sup> Consistent with the finding that tumors with reduced p53 have overexpression of MDM2/MDMX, a major mechanism promoting inactivation of wtp53,<sup>48</sup> KO HSPCs had increased levels of MDM2 (Figure 5D). Thus, *Asrij* is essential for controlling levels of the CSN5-MDM2 axis to maintain p53 levels.

Similar to mouse fibroblasts,<sup>49</sup> in HSPCs, CSN5 localizes to the nucleus as well as the cytoplasm (Figure 5E). Analysis of multiple confocal planes showed significantly increased colocalization of *Asrij* and CSN5 in the cytoplasm as compared with the nucleus (4'-6-diamidino-2-phenylindole [DAPI] stained) (Figure 5E). To explore the possibility of a more direct connection between *Asrij* and CSN5/MDM2/p53, we performed immunopulldown of endogenous *Asrij* in wild-type BM cells and found interaction with CSN5 but not with MDM2 or p53 (Figure 5F). The N-terminal OCIA domain of *Asrij* interacts with several proteins including STAT3 and ARF1 and is necessary and sufficient for *Asrij* function.<sup>14,23,50</sup> To identify the region of *Asrij* that mediates interaction with CSN5, we performed immunoprecipitation on human embryonic kidney 293 (HEK293) cells expressing FLAG-tagged mouse *Asrij* N-terminal fragment that contains the OCIA domain (1-132 aa) or the C-terminal fragment excluding the domain (133-247 aa).<sup>23</sup> CSN5 coimmunoprecipitated with the *Asrij* N-terminal, but not the C-terminal (Figure 5G). Moreover, forced expression of FLAG-tagged full-length *Asrij* in HEK293 cells (Figure 5H) did not alter *csn5* transcript levels; however, p53 transcript levels were significantly increased (Figure 5I). Additionally, CSN5 protein levels were significantly reduced and p53 protein levels increased, suggesting that ectopic expression of *Asrij* could rescue wtp53 proteolysis (Figure 5J).

### Treating *asrij* KO mice with Nutlin-3 rescues the HSPC expansion phenotype

To confirm that reduced p53 activation or stability contributes to loss of quiescence of KO HSCs, we pharmacologically inhibited p53 degradation and looked for reversal of the HSPC expansion phenotype observed in KO mice. Nutlin-3, a small molecule antagonist of MDM2, inhibits p53-MDM2 interaction, thereby activating p53 signaling in cancer cells.<sup>51</sup> Mice were injected intraperitoneally with 20 mg/kg of Nutlin-3 and assayed for p53 protein levels and HSPC frequencies 24 hours postinjection (Figure 6A). Immunoblotting showed that Nutlin-3 restored p53 levels in KO HSPCs to near control levels (Figure 6B). Further, the increased HSPC frequencies in KO mice were also reduced to control levels (Figure 6C). Thus, restoring p53 expression in *asrij* KO mice rescues the HSPC expansion phenotype (Figure 6D).

## Discussion

To ensure lifelong blood cell production, it is important that HSCs maintain the balance between self-renewal and differentiation. Most hematological malignancies are characterized by

a progressive loss of this balance that eventually leads to increased HSCs and biased lineage differentiation.<sup>52</sup> Dysregulation of tumor suppressor pathways and accumulation of DNA damage are major mechanisms that lead to aberrant hematopoiesis.<sup>53</sup> The tumor suppressor p53 plays critical roles in HSPC maintenance.<sup>54</sup> However, mechanisms governing its stability are incompletely understood. Our analysis of the role of *Asrij* in hematopoiesis revealed a novel component that regulates the p53 degradation machinery in HSPCs.

The normal roles of the OCIAD family members in vertebrates are not known though they are implicated in several pathologies. Hence, we generated a global KO mouse to study the role of *Asrij* in vertebrates and its hematopoietic depletion to understand its role in the blood system, given its reported role in *Drosophila* hematopoiesis. Interestingly, in spite of *Asrij* expression in several tissues, null mice showed no apparent defect in development or fertility. However, there was an increasing effect on hematopoietic tissues with age, the cumulative nature of which, suggests that it is due to perturbed blood cell homeostasis. *Asrij* global or hematopoietic-specific KO, both showed perturbed steady-state hematopoiesis in PB, BM, and spleen. Interestingly, heterozygous mutants developed mild phenotypes, possibly owing to reduced (<50%) *Asrij* expression, suggesting a dose-dependent requirement for *Asrij* in regulating hematopoiesis.

Both in vivo and in vitro experiments show that *asrij* depletion accelerates HSPC expansion and promotes differentiation into granulocyte/macrophage progenitors, inducing a myeloproliferative disorder, at least in part because of increased Akt (S473) and STAT5 (Y694) activation.<sup>55</sup> The expanded HSPC pool retains HSC self-renewal properties as seen by the ability of KO BM to repopulate irradiated recipients in serial BMT experiments. However, the BM niche is not *Asrij*-dependent because reciprocal BMT shows that the mutant niche can support hematopoiesis. Taken together, these data indicate that reduced quiescence of KO HSCs is a cell-intrinsic property and not from an unsupportive microenvironment. Further, HSPCs from *asrij*<sup>CKO</sup> mice show similar properties, confirming its role in HSPCs. Additional studies will be required to dissect *Asrij* function, if any, in the BM microenvironment.

Radiation or chemical-induced stress revealed that the expanded HSPC and myeloid pools in *asrij* KO mice do not confer protection but reduce response to stress and lifespan. The unusual results obtained from BMT and irradiation/5-FU treatment assays could be because of differences in the nature of the stress and the niche in which KO HSCs are placed in each case. Additionally, it could also be due to the differential regulation of cell cycle of HSCs under steady state and stressed conditions. Thus, *Asrij* is essential for mediating recovery of the hematopoietic system to maintain homeostasis and its depletion impairs the ability for sustained hematopoiesis. Interestingly, key mediators of inflammation such as Akt, STAT5, and CSN5<sup>56-58</sup> are upregulated in KO from younger ages, before the overt cellular phenotype sets in. This suggests a role for *Asrij* in controlling inflammation stress that merits further investigation. The increasing severity of KO phenotypes with age and the myeloid bias is reminiscent of several human myeloproliferative neoplasms (MPNs).<sup>59</sup> Further, this suggests that as with the *csn5* and *runx3* mutant mouse models,<sup>42,60</sup> *asrij* KO is also an important model of late onset MPNs. However, unlike *csn5* and *runx3* global mutants that are

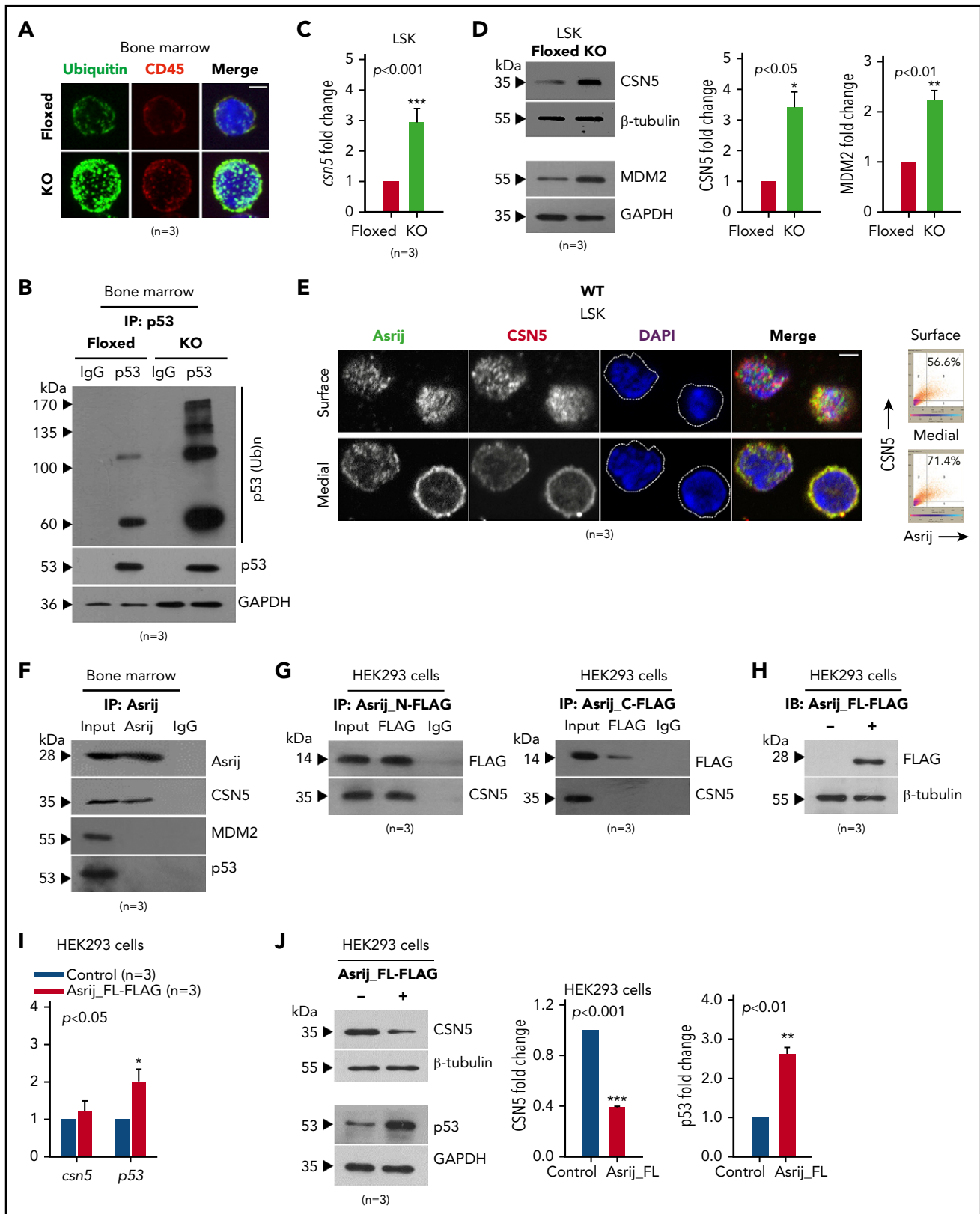


**Figure 5. Asrij interacts with and regulates CSN5 to maintain p53 levels in the BM.** (A-D) Floxed and KO cells from 2-month-old mice were compared in all cases and are indicated in red and light green, respectively. (A) Immunostaining shows increased accumulation of polyubiquitinated proteins in KO BM cells compared with floxed controls ( $n = 30$  cells from 3 mice per genotype). Maximum intensity projection of confocal microscopy images. (B) IP of endogenous p53 from whole BM shows increased levels of polyubiquitinated p53 in KO compared with *asrij* floxed. (C) RT-qPCR analysis for *csn5* transcript levels in HSPCs ( $n = 3$  mice per genotype). (D) Immunoblot analysis and quantification of CSN5 and MDM2 levels in HSPCs ( $n = 3$  mice per genotype). (E) Surface and medial confocal planes of the same cell showing localization of Asrij (green) and CSN5 (red) in HSPCs ( $n = 30$  cells from 3 mice per genotype). White dotted line marks the cell boundary. Plots show percent colocalization in surface and medial planes. (F) IP of

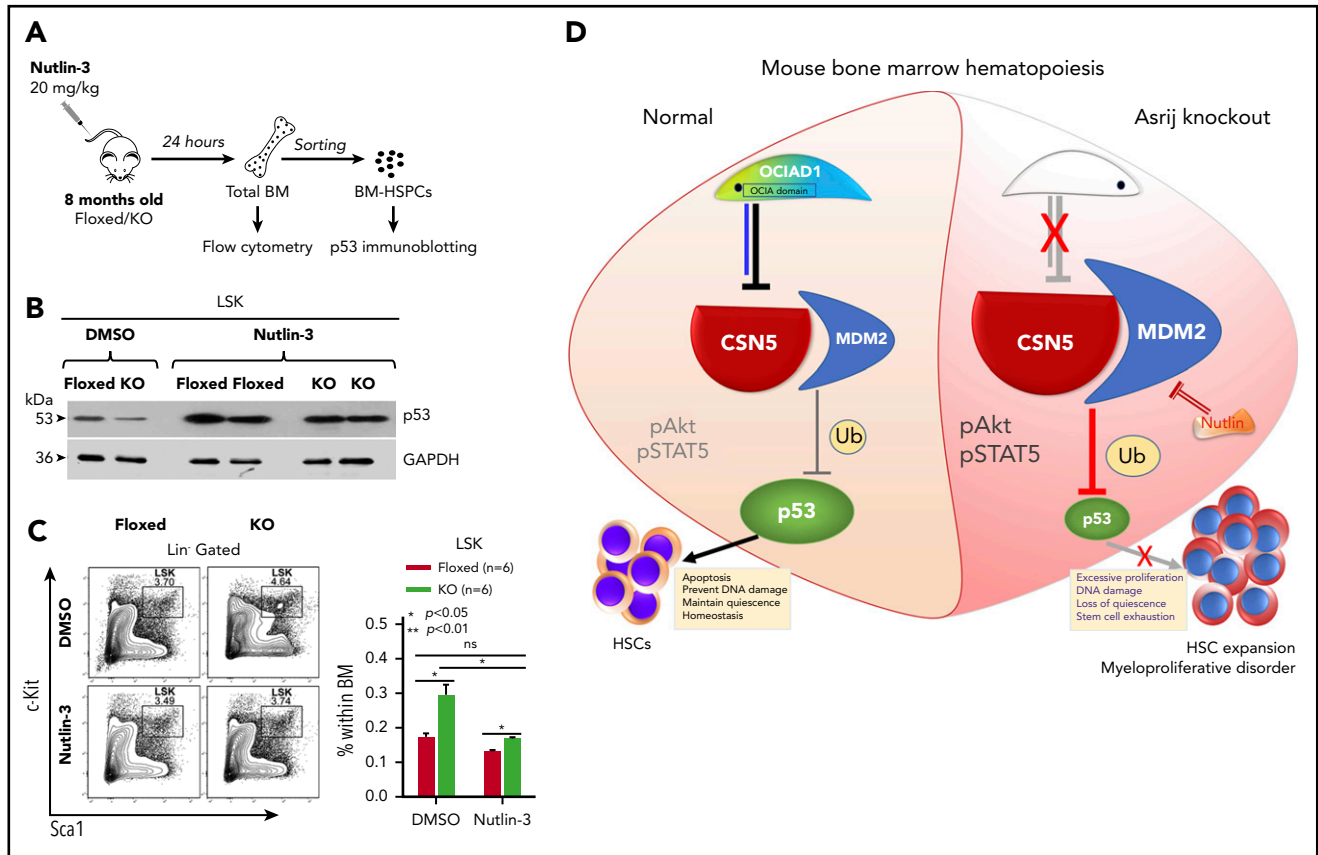


**Figure 6. Nutlin-3 treatment activates p53 and corrects the aberrant HSPC expansion of *asrij* KO mice.** (A) Schematic showing protocol followed for Nutlin-3 treatment of mice and their subsequent analyses. Eight-month-old *asrij* floxed and KO mice were injected intraperitoneally with 20 mg/kg of Nutlin-3 and then analyzed for p53 activation by immunoblotting and HSPC frequencies by flow cytometry. (B) Immunoblot analysis of HSPCs shows increased wtp53 levels in Nutlin-3 treated mice compared with DMSO-treated controls in floxed and KO genotypes ( $n = 4$  per genotype). Loading control: GAPDH. (C) Representative flow cytometry plots and graph show that Nutlin-3 reduces the increased HSPC frequencies observed in KO mice to near control levels ( $n = 6$  per genotype). (D) Model representing mechanism of action of *Asrij* that regulates HSC quiescence. Blue solid line indicates protein interaction. Statistically significant differences in HSPC frequencies determined using ANOVA: single factor analysis are indicated. Error bars denote standard error of mean. \* $P < .05$  and \*\*\* $P < .001$ .

not viable,<sup>60,61</sup> *asrij* KO is viable and fertile, making it a more relevant and versatile model for understanding human MPNs.

Inactivating mutations and deletions in p53 are implicated in >50% of human solid tumors,<sup>62-65</sup> but infrequently in hematological malignancies.<sup>66-70</sup> Moreover, p53 expression is absent or reduced in human myeloid leukemia cell lines.<sup>71</sup> Although the mechanism for p53 silencing in many such cases remains unknown, this is an important factor contributing to cancer progression.<sup>71</sup> Our work unveils several possible mechanisms that could be causing aberrant HSC expansion, including wtp53 dysfunction. *Asrij* positively regulates wtp53 levels to maintain the HSPC pool. In its absence, wtp53 degradation increases, which partly contributes to the abnormal HSPC proliferation accompanied by reduced apoptosis, correlating with reduced *puma* and *noxa* expression. Additionally, the increased levels of polyubiquitinated proteins in *asrij* KO BM cells (suggesting impaired activity of the ubiquitin-proteasome system) and increased Akt/STAT5 activation could also be contributing to the

aberrant hematopoietic phenotypes. Increased proliferation and DNA damage strongly suggest that *Asrij* regulates HSPCs under conditions of replicative stress. This could explain the increased susceptibility of KO mice to genotoxic and chemical stress, which are normally overcome by controlled self-renewal of quiescent HSCs and progenitor proliferation to replenish the depleted BM. Under conditions of stress, loss of *Asrij* leads to uncontrolled proliferation and premature stem cell exhaustion.

The *asrij* KO phenotypes are strikingly similar to those of CSN5 transgenic mice. Although CSN5 antagonizes *Trp53* transcription,<sup>47</sup> *Trp53* transcript levels in KO HSPCs remain unaffected. *Asrij* interacts with CSN5 and negatively regulates its transcript and protein expression. Further, because *Asrij* does not interact with MDM2 or p53, it provides means for distant control of signals that regulate p53 ubiquitination and degradation.

The multifunctionality of CSN5 is often attributed to its dual sub-cellular localization, ability to shuttle between the nucleus and

**Figure 5 (continued)** endogenous *Asrij* in BM lysates from 2-month-old mice shows interaction with CSN5 but not with MDM2 or p53. (G-J) Lysates from HEK293 cells expressing FLAG-tagged *Asrij* constructs. (G) *Asrij* N- and C-terminal fragments were subjected to FLAG IP and probed for interaction with CSN5. At least 2 independent IP experiments were performed with similar results. (H-J) *Asrij*\_FL-FLAG expressing cells (H) validated for FLAG expression by immunoblotting ( $n = 3$ ), and for CSN5, MDM2, and p53 (I) transcript (J) and protein expression, as indicated. (A-E) Nuclei stained with DAPI (blue) and bars represent 2  $\mu$ m. Statistically significant differences in transcript and protein levels determined using ANOVA: single factor analysis are indicated. Error bars denote standard error of mean. \* $P < .05$ , \*\* $P < .01$  and \*\*\* $P < .001$ . IP, immunoprecipitation.

cytoplasm, and mediate cellular functions independent of the COP9 signalosome complex.<sup>18,19</sup> Immunolocalization analysis suggests that the interaction between CSN5 and *Asrij* may be primarily in the cytoplasm. Our results provide new leads to investigate nonnuclear regulation by CSN5 in HSPCs. We propose that just as *Asrij* integrates multiple signaling pathways such as JAK/STAT,<sup>23</sup> Notch,<sup>24</sup> and phosphatidylinositol 3-kinase/Akt<sup>50</sup> pathways in *Drosophila* hematopoiesis, it may similarly integrate multiple inputs in BM hematopoiesis. STAT5 is constitutively activated in several hematopoietic tumors<sup>55</sup> and aberrant phosphatidylinositol 3-kinase/AKT activation is seen in most AML cases with *wtp53* dysfunction via MDM2 activation.<sup>72</sup> Increased Akt/STAT5 activation negatively regulates p53 expression.<sup>73,74</sup> Thus, *Asrij* may regulate the extent of MDM2-mediated *wtp53* ubiquitination and degradation in HSPCs, in multiple ways such as determining CSN5 availability or Akt/STAT5 activation. Loss of this important additional check on mediators of *wtp53* degradation could be one important reason why cancers arise in the absence of p53 mutation.

Targeted activation of dysfunctional *wtp53* may potentially improve treatment of hematological malignancies characterized by reduced p53 levels. Rescue of the KO HSPC expansion phenotype by Nutlin-3 treatment reinforces that *Asrij* functions upstream of p53 for HSPC maintenance. Further, mild phenotypes in the heterozygous KO suggest that *Asrij* tunes the degradation machinery in a dose-dependent manner, to regulate p53 levels posttranscriptionally. Stabilization and activation of p53 also depends on numerous factors such as cellular stress, hypoxia, and metabolic changes. Whether these factors are affected in KO HSPCs needs additional investigation.

Apart from perturbed *Asrij* expression, missense mutations in its OCIA domain have also been reported in patients suffering from chronic lymphocytic leukemia (residue: F45L)<sup>16</sup> and B-cell lymphoma (residue: A119E).<sup>17</sup> Interestingly, although *Asrij* has been implicated in a variety of human cancers, KO mice mostly developed a hematopoietic disorder, possibly because the relatively high turnover of BM cells makes them more susceptible to the effects of reduced p53. This may also be because *Asrij* lies mostly under the transcriptional control of factors such as Runx1, GATA1, Spi1/PU.1, Myc, and Fos, which have well-defined roles in hematopoiesis (<http://codex.stemcells.cam.ac.uk/>).<sup>75</sup> The role of *Asrij*, if any, in fetal hematopoiesis or other tissue-specific stem cells remains to be tested.

In summary, *asrij* KO mice provide a valuable tool to unravel novel mechanisms that drive malignant transformation of HSPCs in the absence of *Trp53* mutations. Patients with myelodysplastic syndromes have increased *csn5* expression and reduced levels of *p53* and *asrij*,<sup>76</sup> which correlates with results obtained from

experiments with *asrij* KO mice, making our findings clinically relevant. Our study supports a requirement for including p53 functional diagnostics<sup>14</sup> to achieve precise treatment of leukemias. Pathologies characterized by *wtp53* dysfunction could be treated by pharmacologically activating context-dependent upstream modulators, such as *Asrij*.

## Acknowledgments

The authors thank Asok Mukhopadhyay, National Institute of Immunology, for CD45.1 and CD45.2 mice; Abhishek Sinha for the FLAG-tagged reporter construct expressing mouse *Asrij*; Abhilash Lakshman for help with repeated measures ANOVA and Kaplan-Meier survival analyses; the anonymous reviewers for their careful reading and insightful comments; Bertie Gottgens for help with data analysis; JNCASR and NCBS Imaging; instrumentation and animal facilities, and Inamdar laboratory members for fruitful discussions.

This work was funded by grants from Indo-French Centre for the Promotion of Advanced Research and intramural funds from DBT-JNCASR "Life Science Research Education and Training" project. NCBS Animal Facility is partially supported by DBT National Mouse Research Resource grant (BT/PR5981/MED/31/181/2012,2013-2016).

## Authorship

Contribution: M.S.I. conceived the project; M.S.I., T.A., H.K., and K.V. designed the strategy for generation of *asrij* knockout mice; S.S., M.S.I., T.A., H.K., T.R.D., R.Y., and V.A.B. performed research and collected data; S.S., T.R.D., and M.S.I. analyzed and interpreted data, performed statistical analysis, and prepared figures; S.S. and M.S.I. wrote the manuscript.

Conflict-of-interest disclosure: The authors declare no competing financial interests.

ORCID profile: M.S.I., 0000-0002-8243-2821.

Correspondence: Maneesha S. Inamdar, Jawaharlal Nehru Centre for Advanced Scientific Research, Jakkur P.O., Bangalore 560064, India; e-mail: inamdar@jncasr.ac.in.

## Footnotes

Submitted 10 December 2018; accepted 18 March 2019. Prepublished online as *Blood* First Edition paper, 5 April 2019; DOI 10.1182/blood.2019000530.

Please e-mail the corresponding author regarding requests for original data (see supplemental Methods for additional information.)

The online version of this article contains a data supplement.

The publication costs of this article were defrayed in part by page charge payment. Therefore, and solely to indicate this fact, this article is hereby marked "advertisement" in accordance with 18 USC section 1734.

## REFERENCES

- Hemmati S, Haque T, Gritsman K. Inflammatory signaling pathways in preleukemic and leukemic stem cells. *Front Oncol*. 2017;7:265.
- Adair JE, Kubek SP, Kiem HP. Hematopoietic stem cell approaches to cancer. *Hematol Oncol Clin North Am*. 2017;31(5):897-912.
- Tamma R, Ribatti D. Bone niches, hematopoietic stem cells, and vessel formation. *Int J Mol Sci*. 2017;18(1):E151.
- Woolthuis CM, Park CY. Hematopoietic stem/progenitor cell commitment to the megakaryocyte lineage. *Blood*. 2016;127(10):1242-1248.
- Geiger H, de Haan G, Florian MC. The ageing haematopoietic stem cell compartment. *Nat Rev Immunol*. 2013;13(5):376-389.
- Elias HK, Bryder D, Park CY. Molecular mechanisms underlying lineage bias in aging hematopoiesis. *Semin Hematol*. 2017;54(1):4-11.
- Venezia TA, Merchant AA, Ramos CA, et al. Molecular signatures of proliferation and quiescence in hematopoietic stem cells. *PLoS Biol*. 2004;2(10):e301.
- Forsberg EC, Prohaska SS, Katzman S, Heffner GC, Stuart JM, Weissman IL. Differential expression of novel potential regulators in hematopoietic stem cells. *PLoS Genet*. 2005;1(3):e28.
- Pant V, Quintás-Cardama A, Lozano G. The p53 pathway in hematopoiesis: lessons from mouse models, implications for humans. *Blood*. 2012;120(26):5118-5127.

10. Rivlin N, Brosh R, Oren M, Rotter V. Mutations in the p53 tumor suppressor gene: important milestones at the various steps of tumorigenesis. *Genes Cancer*. 2011;2(4):466-474.
11. Asai T, Liu Y, Bae N, Nimer SD. The p53 tumor suppressor protein regulates hematopoietic stem cell fate. *J Cell Physiol*. 2011;226(9):2215-2221.
12. Petitjean A, Mathe E, Kato S, et al. Impact of mutant p53 functional properties on TP53 mutation patterns and tumor phenotype: lessons from recent developments in the IARC TP53 database. *Hum Mutat*. 2007;28(6):622-629.
13. Bouaoun L, Sonkin D, Ardin M, et al. TP53 variations in human cancers: new lessons from the IARC TP53 database and genomics data. *Hum Mutat*. 2016;37(9):865-876.
14. Prokocimer M, Molchadsky A, Rotter V. Dysfunctional diversity of p53 proteins in adult acute myeloid leukemia: projections on diagnostic workup and therapy. *Blood*. 2017;130(6):699-712.
15. Meek DW, Anderson CW. Posttranslational modification of p53: cooperative integrators of function. *Cold Spring Harb Perspect Biol*. 2009;1(6):a000950.
16. Landau DA, Carter SL, Stojanov P, et al. Evolution and impact of subclonal mutations in chronic lymphocytic leukemia. *Cell*. 2013;152(4):714-726.
17. Morin RD, Assouline S, Alcaide M, et al. Genetic landscapes of relapsed and refractory diffuse large B-cell lymphomas. *Clin Cancer Res*. 2016;22(9):2290-2300.
18. Bagger FO, Sasivarevic D, Sohi SH, et al. BloodSpot: a database of gene expression profiles and transcriptional programs for healthy and malignant haematopoiesis. *Nucleic Acids Res*. 2016;44(D1):D917-D924.
19. Bao F, LoVerro PR, Fisk JN, Zhurkin VB, Cui F. p53 binding sites in normal and cancer cells are characterized by distinct chromatin context. *Cell Cycle*. 2017;16(21):2073-2085.
20. Povlsen LK, Beli P, Wagner SA, et al. Systems-wide analysis of ubiquitylation dynamics reveals a key role for PAF15 ubiquitylation in DNA-damage bypass. *Nat Cell Biol*. 2012;14(10):1089-1098.
21. Sinha S, Bheemsetty VA, Inamdar MS. A double helical motif in OCIAD2 is essential for its localization, interactions and STAT3 activation. *Sci Rep*. 2018;8(1):7362.
22. Mukhopadhyay A, Das D, Inamdar MS. Embryonic stem cell and tissue-specific expression of a novel conserved gene, asrij. *Dev Dyn*. 2003;227(4):578-586.
23. Sinha A, Khadilkar RJ, S VK, Roychowdhury Sinha A, Inamdar MS. Conserved regulation of the Jak/STAT pathway by the endosomal protein asrij maintains stem cell potency. *Cell Reports*. 2013;4(4):649-658.
24. Kulkarni V, Khadilkar RJ, Magadi SS, Inamdar MS. Asrij maintains the stem cell niche and controls differentiation during *Drosophila* lymph gland hematopoiesis [published correction appears in *PLoS One*. 2012;7(4)]. *PLoS One*. 2011;6(11):e27667.
25. Schwenk F, Baron U, Rajewsky K. A transgenic mouse strain for the ubiquitous deletion of loxP-flanked gene segments including deletion in germ cells. *Nucleic Acids Res*. 1995;23(24):5080-5081.
26. Siegemund S, Shepherd J, Xiao C, Sauer K. hCD2-iCre and Vav-iCre mediated gene recombination patterns in murine hematopoietic cells. *PLoS One*. 2015;10(4):e0124661.
27. Nestorowa S, Hamey FK, Pijuan Sala B, et al. A single-cell resolution map of mouse hematopoietic stem and progenitor cell differentiation. *Blood*. 2016;128(8):e20-e31.
28. Bibi S, Arslanhan MD, Langenfeld F, et al. Co-operating STAT5 and AKT signaling pathways in chronic myeloid leukemia and mastocytosis: possible new targets of therapy. *Haematologica*. 2014;99(3):417-429.
29. Ito K, Hirao A, Arai F, et al. Regulation of oxidative stress by ATM is required for self-renewal of haematopoietic stem cells. *Nature*. 2004;431(7011):997-1002.
30. Janzen V, Forkert R, Fleming HE, et al. Stem-cell ageing modified by the cyclin-dependent kinase inhibitor p16INK4a. *Nature*. 2006;443(7110):421-426.
31. Maryanovich M, Oberkovitz G, Niv H, et al. The ATM-BID pathway regulates quiescence and survival of haematopoietic stem cells. *Nat Cell Biol*. 2012;14(5):535-541.
32. Shao L, Feng W, Li H, et al. Total body irradiation causes long-term mouse BM injury via induction of HSC premature senescence in an Ink4a- and Arf-independent manner. *Blood*. 2014;123(20):3105-3115.
33. Wang J, Sun Q, Morita Y, et al. A differentiation checkpoint limits hematopoietic stem cell self-renewal in response to DNA damage. *Cell*. 2014;158(6):1444.
34. Del Giudice I, Messina M, Chiaretti S, et al. Behind the scenes of non-nodal MCL: downmodulation of genes involved in actin cytoskeleton organization, cell projection, cell adhesion, tumour invasion, TP53 pathway and mutated status of immunoglobulin heavy chain genes. *Br J Haematol*. 2012;156(5):601-611.
35. Akala OO, Park IK, Qian D, Pihalja M, Becker MW, Clarke MF. Long-term hematopoietic reconstitution by Trp53<sup>-/-</sup>p16Ink4a<sup>-/-</sup>p19Arf<sup>-/-</sup> multipotent progenitors. *Nature*. 2008;453(7192):228-232.
36. Chen J, Ellison FM, Keyvanfar K, et al. Enrichment of hematopoietic stem cells with SLAM and LSK markers for the detection of hematopoietic stem cell function in normal and Trp53 null mice. *Exp Hematol*. 2008;36(10):1236-1243.
37. Liu Y, Elf SE, Miyata Y, et al. p53 regulates hematopoietic stem cell quiescence. *Cell Stem Cell*. 2009;4(1):37-48.
38. TeKippe M, Harrison DE, Chen J. Expansion of hematopoietic stem cell phenotype and activity in Trp53-null mice. *Exp Hematol*. 2003;31(6):521-527.
39. Williams AB, Schumacher B. p53 in the DNA-damage-repair Process. *Cold Spring Harb Perspect Med*. 2016;6(5):a026070.
40. Pant V, Lozano G. Limiting the power of p53 through the ubiquitin proteasome pathway. *Genes Dev*. 2014;28(16):1739-1751.
41. Yang Y, Li CC, Weissman AM. Regulating the p53 system through ubiquitination. *Oncogene*. 2004;23(11):2096-2106.
42. Mori M, Yoneda-Kato N, Yoshida A, Kato JY. Stable form of JAB1 enhances proliferation and maintenance of hematopoietic progenitors. *J Biol Chem*. 2008;283(43):29011-29021.
43. Wei N, Deng XW. The COP9 signalosome. *Annu Rev Cell Dev Biol*. 2003;19(1):261-286.
44. Schwegheimer C. The COP9 signalosome (CSN): an evolutionary conserved proteolytic regulator in eukaryotic development. *Biochim Biophys Acta*. 2004;1695(1-3):45-54.
45. Li L, Deng XW. The COP9 signalosome: an alternative lid for the 26S proteasome? *Trends Cell Biol*. 2003;13(10):507-509.
46. Bech-Otschir D, Kraft R, Huang X, et al. COP9 signalosome-specific phosphorylation targets p53 to degradation by the ubiquitin system. *EMBO J*. 2001;20(7):1630-1639.
47. Zhang XC, Chen J, Su CH, Yang HY, Lee MH. Roles for CSN5 in control of p53/MDM2 activities. *J Cell Biochem*. 2008;103(4):1219-1230.
48. Toledo F, Wahl GM. MDM2 and MDM4: p53 regulators as targets in anticancer therapy. *Int J Biochem Cell Biol*. 2007;39(7-8):1476-1482.
49. Tomoda K, Kubota Y, Arata Y, et al. The cytoplasmic shuttling and subsequent degradation of p27Kip1 mediated by Jab1/CSN5 and the COP9 signalosome complex. *J Biol Chem*. 2002;277(3):2302-2310.
50. Khadilkar RJ, Rodrigues D, Mote RD, et al. ARF1-GTP regulates Asrij to provide endocytic control of *Drosophila* blood cell homeostasis. *Proc Natl Acad Sci USA*. 2014;111(13):4898-4903.
51. Villalonga-Planells R, Coll-Mulet L, Martínez-Soler F, et al. Activation of p53 by nutlin-3a induces apoptosis and cellular senescence in human glioblastoma multiforme. *PLoS One*. 2011;6(4):e18588.
52. Akunuru S, Geiger H. Aging, clonality, and rejuvenation of hematopoietic stem cells. *Trends Mol Med*. 2016;22(8):701-712.
53. Li T, Zhou ZW, Ju Z, Wang ZQ. DNA damage response in hematopoietic stem cell ageing. *Genomics Proteomics Bioinformatics*. 2016;14(3):147-154.
54. Liu Y, Elf SE, Asai T, et al. The p53 tumor suppressor protein is a critical regulator of hematopoietic stem cell behavior. *Cell Cycle*. 2009;8(19):3120-3124.
55. Kato Y, Iwama A, Tadokoro Y, et al. Selective activation of STAT5 unveils its role in stem cell self-renewal in normal and leukemic hematopoiesis. *J Exp Med*. 2005;202(1):169-179.
56. Tang B, Tang F, Wang Z, et al. Upregulation of Akt/NF- $\kappa$ B-regulated inflammation and Akt/Bad-related apoptosis signaling pathway involved in hepatic carcinoma process: suppression by casomix acid nanoparticle. *Int J Nanomedicine*. 2016;11:6401-6420.
57. Lim SO, Li CW, Xia W, et al. Deubiquitination and stabilization of PD-L1 by CSN5. *Cancer Cell*. 2016;30(6):925-939.

58. Meynard D, Sun CC, Wu Q, et al. Inflammation regulates TMPRSS6 expression via STAT5. *PLoS One*. 2013;8(12):e82127.
59. Levine RL, Pardanani A, Tefferi A, Gilliland DG. Role of JAK2 in the pathogenesis and therapy of myeloproliferative disorders. *Nat Rev Cancer*. 2007;7(9):673-683.
60. Wang CQ, Motoda L, Satake M, et al. Runx3 deficiency results in myeloproliferative disorder in aged mice. *Blood*. 2013;122(4):562-566.
61. Tomoda K, Yoneda-Kato N, Fukumoto A, Yamanaka S, Kato JY. Multiple functions of Jab1 are required for early embryonic development and growth potential in mice. *J Biol Chem*. 2004;279(41):43013-43018.
62. Vogelstein B, Lane D, Levine AJ. Surfing the p53 network. *Nature*. 2000;408(6810):307-310.
63. Vousden KH, Prives C. Blinded by the light: the growing complexity of p53. *Cell*. 2009;137(3):413-431.
64. Brady CA, Attardi LD. p53 at a glance. *J Cell Sci*. 2010;123(Pt 15):2527-2532.
65. Muller PA, Vousden KH. p53 mutations in cancer. *Nat Cell Biol*. 2013;15(1):2-8.
66. Lens D, De Schouwer PJ, Hamoudi RA, et al. p53 abnormalities in B-cell prolymphocytic leukemia. *Blood*. 1997;89(6):2015-2023.
67. Stirewalt DL, Kopecky KJ, Meshinchi S, et al. FLT3, RAS, and TP53 mutations in elderly patients with acute myeloid leukemia. *Blood*. 2001;97(11):3589-3595.
68. Newcomb EW. P53 gene mutations in lymphoid diseases and their possible relevance to drug resistance. *Leuk Lymphoma*. 1995;17(3-4):211-221.
69. Wattel E, Preudhomme C, Hecquet B, et al. p53 mutations are associated with resistance to chemotherapy and short survival in hematologic malignancies. *Blood*. 1994;84(9):3148-3157.
70. Lionetti M, Barbieri M, Manzoni M, et al. Molecular spectrum of TP53 mutations in plasma cell dyscrasias by next generation sequencing: an Italian cohort study and overview of the literature. *Oncotarget*. 2016;7(16):21353-21361.
71. Durland-Busbice S, Reisman D. Lack of p53 expression in human myeloid leukemias is not due to mutations in transcriptional regulatory regions of the gene. *Leukemia*. 2002;16(10):2165-2167.
72. Wade M, Li YC, Wahl GM. MDM2, MDMX and p53 in oncogenesis and cancer therapy. *Nat Rev Cancer*. 2013;13(2):83-96.
73. Ogawara Y, Kishishita S, Obata T, et al. Akt enhances Mdm2-mediated ubiquitination and degradation of p53. *J Biol Chem*. 2002;277(24):21843-21850.
74. Ren Z, Aerts JL, Vandenplas H, et al. Phosphorylated STAT5 regulates p53 expression via BRCA1/BARD1-NPM1 and MDM2. *Cell Death Dis*. 2016;7(12):e2560.
75. Sánchez-Castillo M, Ruau D, Wilkinson AC, et al. CODEX: a next-generation sequencing experiment database for the haematopoietic and embryonic stem cell communities. *Nucleic Acids Res*. 2015;43(Database issue):D1117-D1123.
76. Haferlach T, Kohlmann A, Wiczorek L, et al. Clinical utility of microarray-based gene expression profiling in the diagnosis and subclassification of leukemia: report from the International Microarray Innovations in Leukemia Study Group. *J Clin Oncol*. 2010;28(15):2529-2537.